LETTER

Efficient carpet invisibility cloaking with dielectric resonant metasurfaces in terahertz region

IOP Publishing | Astro Ltd Laser Physics Letters
Laser Phys. Lett. **18** (2021) 026201 (6pp) https://doi.org/10.1088/1612-202X/abd5b3

Letter

Efficient carpet invisibility cloaking with dielectric resonant metasurfaces in terahertz region

Tian Lu[1], Dantian Feng[1,2], Bo Fang[3], Pengwei Zhou[1,4], Dong Yao[4], Xufeng Jing[1,2], Chenxia Li[1], Haiyong Gan[5], Yingwei He[5], Jinhui Cai[3] and Zhi Hong[2]

[1] Institute of Optoelectronic Technology, China Jiliang University, Hangzhou 310018, People's Republic of China
[2] Centre for THz Research, China Jiliang University, Hangzhou 310018, People's Republic of China
[3] College of Metrology & Measurement Engineering, China Jiliang University, Hangzhou 310018, People's Republic of China
[4] Key Laboratory of Airborne Optical Imaging and Measurement, Changchun Institute of Optics, Fine Mechanics and Physics, Chinese Academy of Science, Changchun, People's Republic of China
[5] National Institute of Metrology, Beijing, People's Republic of China

E-mail: jingxufeng@cjlu.edu.cn and ganhaiyong@nim.ac.cn

Received 15 December 2020
Accepted for publication 18 December 2020
Published 8 January 2021

Abstract

The application of metasurface in invisibility technology is mainly based on its phase control function, which provides a new choice for the design of ultra-thin carpet cloaking devices with arbitrary shape. At present, most of the carpet cloaking devices mainly focus on metal structure metasurfaces. The Ohmic loss of metallic materials seriously affects the efficiency of cloaking devices. To reduce Ohmic loss and improve reflection efficiency, a dielectric resonance cylindrical harmonic oscillator is proposed to construct the metasurface layer. Based on the analysis of the principle of carpet reflection cloaking, a dielectric metasurface layer is optimized to cover a triangular scatterer, making it invisible. The near field and far field scattering characteristics of dielectric metasurface carpet cloaking device are numerically simulated to confirm its cloaking effect.

Keywords: terahertz wave, metasurface, cloaking, generalized Snell's law

(Some figures may appear in colour only in the online journal)

1. Introduction

Metamaterial is a kind of artificial material with sub wavelength structure, which has extraordinary physical properties that natural materials do not have. It can realize abnormal propagation of light, such as zero refractive index and negative refractive index, super imaging, and so on [1–8]. Recently, metasurface has been proposed as a development version of metamaterials [9–14]. Metasurface can be applied in holography, absorber, metalens, bound-state in continuum, etc [15–19]. Specially, metasurface can be also used in invisible cloaking [11]. The original cloaking devices were designed based on the theory of transform optics [20]. Based on the distribution of complex effective permittivity and permeability designed by transform optics, electromagnetic waves can bypass obstacles and achieve invisible effect. However, the cloaking device requires complex anisotropic metamaterial design and is not easy to implement in experiments.

Subsequently, in order to simplify the design and preparation of cloaking devices, some simple methods have been proposed, such as quasi-conformal mapping [21],

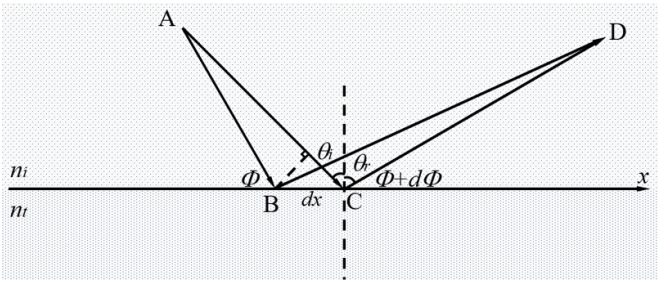

Figure 1. Schematic diagram of generalized Snell's reflection law.

homogeneous coordinate transformation [22], scattering cancellation [23], near-zero refractive index metamaterials [24], and microstrip patch antennas [25], and so on. These devices can produce cloaking effects while having small thicknesses, but usually perform poorly under high-sensitivity detection. Recently, several multiple wavelengths and relatively broadband carpet cloaking have been recently reported [26–30]. Compared with metamaterial cloaking devices, the thickness and complexity of cloaking devices can be significantly reduced by using metasurfaces, which provides a new possibility for the design of light and preparable cloaking devices. Metasurface cloaking devices can be realized by covering a carefully designed ultra-thin metasurface on the surface of an object. The wavefront of reflected or transmitted waves can be properly modulated, resulting in reflection and transmission effects that did not originally exist. However, at present, most of the carpet cloaking devices mainly focus on the metasurfaces with metal structure. The ohmic loss of metal material seriously affects the efficiency of designed devices. In order to reduce ohmic loss and improve the efficiency of cloaking devices, we propose the use of a full dielectric harmonic oscillator metasurface to construct a carpet cloaking in terahertz region.

2. Carpet cloaking principle

The basic principle of the realization of a metasurface carpet cloaking is based on the generalized Snell's law. Generally, if a reflection surface with a specific phase gradient function is obtained, the electromagnetic characteristics such as the phase and propagation direction of the reflected wave can be modulated. For example, the phase of the reflected wave of a convex object is modulated into a phase of reflected wave similar to the case of plane reflection, so as to achieve the cloaking effect of hiding the object below it. Metasurface is one of the important ways to provide a phase gradient function and perform phase modulation of reflected waves.

The schematic diagram of the generalized Snell's law is shown in figure 1. Its basic principle introduces the concept of phase gradient. The two beams of light AB and AC emitted from point A are reflected on the reflective boundary surface of the medium with refractive indexes of n_i and n_t on both sides, respectively, and two reflected beams of BD and CD are generated. According to Fermat's principle, the phase of light

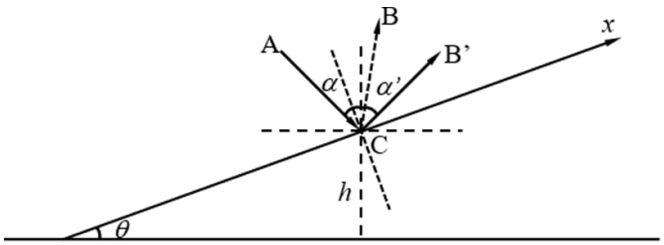

Figure 2. The light is incident on the left inclined slope.

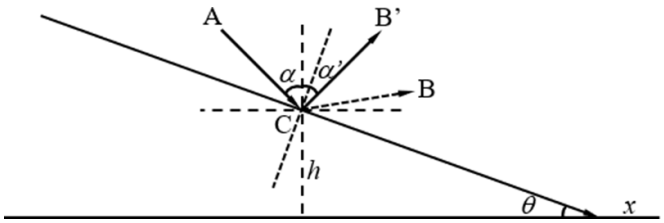

Figure 3. The light is incident on the inclined slope on the right.

reaching the point D through the two paths of ABD and ACD is the same, so it is easy to have

$$k_0 n_i \sin\theta_i \mathrm{d}x + \phi + \mathrm{d}\phi = k_0 n_i \sin\theta_r \mathrm{d}x + \phi \tag{1}$$

where k_0 is the wave number of the incident light and it is

$$k_0 = \frac{2\pi}{\lambda_0} \tag{2}$$

where λ_0 is the wavelength of incident light in vacuum, and one can further obtain as

$$\sin\theta_r - \sin\theta_i = \frac{\lambda_0}{2\pi n_i}\frac{\mathrm{d}\varphi}{\mathrm{d}x} \tag{3}$$

Equation (3) shows the generalized Snell reflection law, where $\frac{\mathrm{d}\phi}{\mathrm{d}x}$ is the phase gradient of the reflection surface. When $\frac{\mathrm{d}\phi}{\mathrm{d}x}$ is zero, equation (3) can be simplified as

$$\theta_r = \theta_i \tag{4}$$

Equation (4) is the conventional Snell's reflection law.

When a beam of light is incident on an inclined slope with a carefully designed phase gradient metasurface on the left of a triangular steep slope, the reflection of the light is anomalous as shown in figure 2. When the light is incident from point A to point C on the inclined slope, the reflected light should be emitted in the direction of CB symmetrical to the normal of the slope without designed phase gradient. When a gradient phase metasurface is introduced, the pre-designed phase shift on the inclined slope can change the partial reflection phase, making the light reflected abnormally. The reflected light is modulated to the direction of CB′, which is symmetrical to the incident light and exits the normal direction of the horizontal plane. At the far-field position, the reflected wave signal detected by a detector is similar to the reflected wave signal of the horizontal plane, that is, the inclined slope and its contents are hidden by the metasurface, and the true object shape

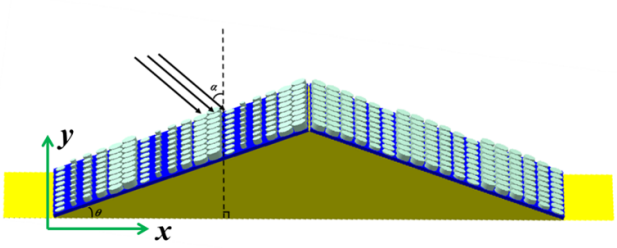

Figure 4. Overall structure of the carpet cloaking device. Inclination angle $\theta = 20°$, center frequency $f = 0.75$ THz, incident angle $\alpha = 45°$.

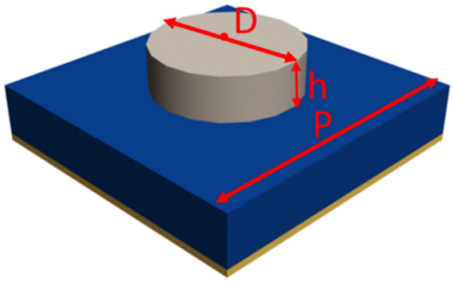

Figure 5. Schematic diagram of the metasurface unit structure.

cannot be detected. The local phase distribution provided by the metasurface cloaking satisfies the following relationship as

$$\delta = \pi - 2hk_0 \cos\alpha \tag{5}$$

where k_0 is the wave vector in free space, h is the height of any point on the surface of the cloaking device from the horizontal ground, and α is the incident angle of incident light.

As shown in figure 3, when a ray of light is incident on the inclined slope covered with a phase gradient metasurface on the right side, the light will also reflect abnormally. The local phase distribution also satisfies equation (5). Thus, when the incident light is incident on the inclined surface, a phase gradient metasurface can provide specific local phase compensation, the reflected wave generated by it can be modulated into a plane wave reflection or an arbitrary designed wave surface reflection shape. The detector cannot detect the true shape of the object, so as to hide the object below the slope.

3. Efficient carpet cloaking with dielectric metasurface structure

Figure 4 shows the designed overall structure of a carpet cloaking device. The overall shape of the designed terahertz wave metasurface device is a symmetrical triangular slope surface structure. The slope angle $\theta = 20°$. The six elements structure acts as a superperiodic structure on the inclined plane. Three superperiodic units are arranged on the left and right sides of the triangular slope at x-direction. At y-direction, nine cycles are arranged. In theory, we could arrange more

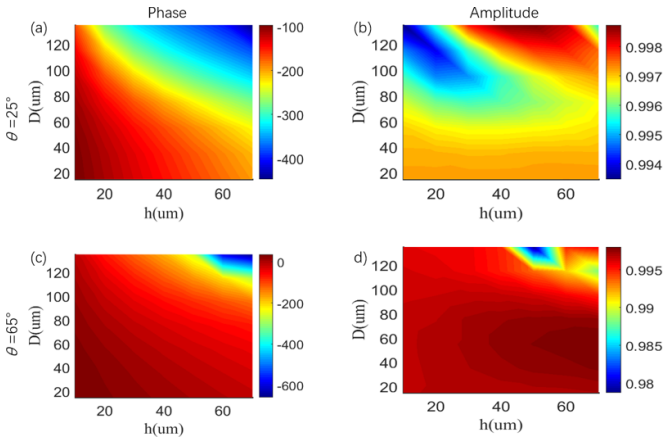

Figure 6. The relationship between amplitude and phase of reflected wave and cylinder dimensions D and h at different incident angles. (a) Left slope $\theta_i' = \alpha - \theta = 25°$, (b) Right slope $\theta_i'' = \alpha + \theta = 65°$.

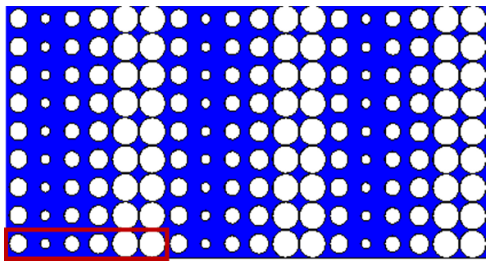

Figure 7. Periodic arrangement of unit structure.

periodic structures so that larger objects could be hidden under triangular slope. In the process of design and calculation, in order to reduce the leakage of the incident electromagnetic wave, we add a layer of metal plates on the bottom and sides of the triangular slope.

The key to the design of a metasurface carpet cloaking device is to obtain a metasurface unit structure that can meet the phase conditions proposed above. The incident angle of the incident electromagnetic wave to the overall structure of the device is $\alpha = 45°$, and the polarization of the incident wave is parallel to the cylindrical surface. The working frequency is designed at $f = 0.75$ THz. It can be known from $c = \lambda f$ that a wave with a frequency of 0.75 THz corresponds to a wavelength of $\lambda_0 = 4 \times 10^{-4}$ m in vacuum. When the overall structure is designed to take six phase gradient units as one cycle, then $\mathrm{d}\phi = 2\pi/6 = \pi/3$. The basic period dimension of the metasurface unit structure is as $P = \mathrm{d}x = \frac{\lambda}{12\sin\theta\cos\alpha} = 138\,\mu$m.

The schematic diagram of the metasurface unit structure is shown in figure 5. The metasurface structure unit can be decomposed into three layers: the bottom layer is a thin aluminum substrate with a thickness of 5 μm. The purpose of using metal as the substrate is to increase the reflectivity. The aluminum substrate is covered with a layer of polyimide film (Polymide (loss free)) with a thickness of 30 μm ($P = 138$ μm). Polyimide film has the advantages of excellent high and low temperature resistance, electrical insulation

Table 1. Phase and amplitude responses of optimized unit structures with different structural parameters.

	Left sidewise ($\theta_i' = \alpha - \theta = 25^\circ$)				Left sidewise ($\theta_i'' = \alpha + \theta = 65^\circ$)			
Unit cell	D	h	Amplitude	Phase	D	h	Amplitude	Phase
1	93.4	10	0.99	−120	120	10	0.99	0
2	50	48.5	0.97	−180	108.3	30	0.99	−60
3	79.5	50	0.94	−240	110	46.3	0.99	−120
4	100	50	0.93	−300	120.8	50	0.99	−180
5	135	43.7	0.95	−360	130	52.1	0.98	−240
6	135	65.9	0.98	−420	130	56.1	0.97	−300

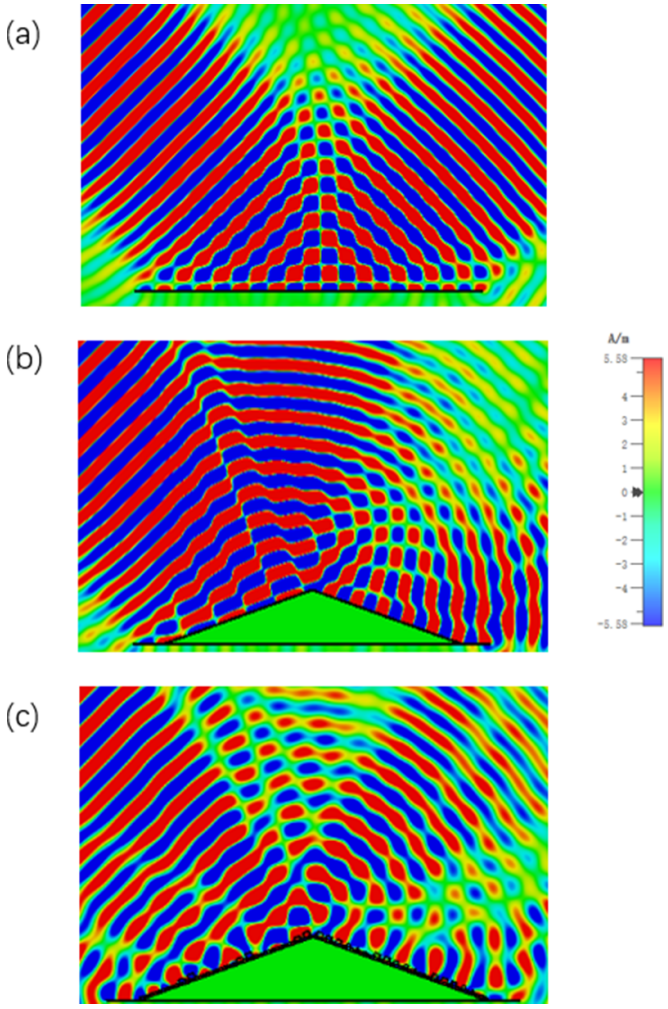

Figure 8. Electric field distributions at 0.75 THz. (a) Ground plane, (b) bare bump, (c) bump covered with metasurface layer.

and dielectric resistance. The top layer is a silicon cylinder, whose diameter D and height h are variables. By changing D and h at the same time to achieve different phase transitions of the cell structure, and then build a phase gradient metasurface to achieve invisible function. That is, by adjusting the shape of the top cylinder in the unit structure, the phase of the reflected wave can be changed while ensuring that its amplitude is sufficiently high. In order to calculate the phase shift from a single metasurface element structure, we assume that its response can be approximately an infinite periodic array. In our design, the cylinder is made of materials with high dielectric constant, which can concentrate the electric field and the coupling between the elements is weak, so each element can be regarded as independent unit. In addition, due to the small phase gradient, there is little difference in the size of the adjacent cylinders. Therefore, the total electromagnetic field of the whole cloaking device can be regarded as the superposition of the field of each unit structure.

Next, we will optimize six cell structures, and their phase response coverage reaches 2π. The phase difference between the adjacent cell structures is $\pi/3$. The terahertz wave with the center frequency of 0.75 Thz is incident at an angle of $\alpha = 45^\circ$ with respect to the horizontal plane. According to the geometric relationship in figure 2, the actual incident angle of light should be $\theta_i' = \alpha - \theta = 25^\circ$ for the left slope, and $\theta_i'' = \alpha + \theta = 65^\circ$ for the right slope. Therefore, it is necessary to find out the parameters D and h that can meet the phase compensation conditions when the actual incident angle is 25° and 65°, respectively, and then they are tiled on the left and right slopes according to a certain phase gradient. At this time, when the terahertz wave is incident at 45°, the designed metasurface cloaking device can reflect the incident wave to the 45° direction, which realizes the effect of quasi plane reflection, that is, the slope surface is hidden. The phase and amplitude of reflection wave are shown in figure 6 at the different incident angle. The finite integral method is used to optimize the height and diameter of the cylinder structure. Based on figure 6, the optimized dimensions of the six cell structures are shown in table 1. The six optimized cell structures are arranged to construct the metasurface. The top view of the arrangement of metasurface unit cells is shown in figure 7.

In order to prove the cloaking effect of the designed metasurface carpet cloaking device, the electromagnetic field distribution is simulated numerically by the finite integral method. In order to compare the stealth effect clearly, we simulate the near-field distribution of metal flat plates and triangular structures without cloaks. The incident frequency is at 0.75 THz with the incident angle of 45°. Figure 8(a) corresponds to the near-field electric field intensity distribution of plane reflected wave. Figure 8(b) corresponds to the near-field electric field intensity distribution of reflection wave of bare triangular slop. Figure 8(c) corresponds to the near-field electric field intensity distribution of reflected wave of cloaking device with metasurface. Combined with the three cases in figure 8,

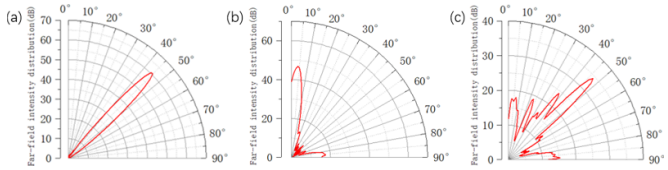

Figure 9. Far-field intensity distributions at 0.75 THz. (a) Ground plane, (b) bare bump, (c) bump covered with metasurface layer.

it can be observed that the wavefront of the reflected wave generated by terahertz wave irradiating the bare device has obvious distortion. After the designed metasurface is covered on it, the reflected wave front is well recovered as a plane wave reflecting off a metal plate.

Figure 9 shows the far-field scattering intensity distribution in three cases. Compared with the three cases in figure 9, it can be clearly observed that the far-field scattering intensity distribution of the bare device is obviously different from that of cloaking device covered a metasurface layer. In figure 9(c), the overall scattering intensity distribution is similar to the plane reflection in figure 9(a). The reflected wave energy can be mainly concentrated in the 45° plane reflection direction and the far-field direction can be detected. The detector cannot recognize its specific shape information, and it achieves good stealth effect. However, for the bare device without metasurface, under the same conditions, the near-field electric field intensity distribution of the reflected wave conforms to the Snell reflection law. Two oblique surfaces act on the incident electromagnetic wave respectively and produce two beams of reflected waves in different directions.

4. Conclusions

In order to improve the reflection efficiency and reduce the ohmic loss, we propose a dielectric cylindrical structure to construct the metasurface. Based on the analysis of the principle of reflective carpet cloaking, a dielectric metasurface cloaking device was proposed. The terahertz wave multilayer metasurface cloaking device designed in this paper has good invisible effect when the electromagnetic wave is incident at the frequency of 0.75 THz and the incident angle of 45°. The near and far field characteristics are numerically simulated to demonstrate the cloaking effect.

Acknowledgments

Funded by the Open Foundation of the Key Laboratory of Aeronautical Optical Imaging and Measurement, Chinese Academy of Sciences, Project 62075202 supported by National Natural Science Foundation of China, Project LY20F050008 supported by Natural Science Foundation of Zhejiang Province. Natural Science Foundation of Zhejiang Province (Nos. LZ21A040003, LY20F050007); National Natural Science Foundation of China (NSFC) (No. 61875179).

References

[1] He X and Lu H 2014 Graphene-supported tunable extraordinary transmission *Nanotechnology* **25** 325201
[2] He X 2015 Tunable terahertz graphene metamaterials *Carbon* **82** 229–37
[3] Guan H, Chen H, Wu J, Jin Y, Kong F, Liu S, Yi K and Shao J 2014 High-efficiency broad-bandwidth metal/multilayer-dielectric gratings *Opt. Lett.* **39** 170–3
[4] He X, Zhong X, Lin F and Shi W 2016 Investigation of graphene assisted tunable terahertz metamaterials absorber *Opt. Mater. Express* **6** 331–42
[5] Luo X, Tan Z, Wang C and Cao J 2019 A reflecting-type highly efficient terahertz cross-polarization converter based on metamaterials *Chin. Opt. Lett.* **17** 093101
[6] Liang W, Li Z, Wang Y, Chen W and Li Z 2019 All-angle optical switch based on the zero reflection effect of graphene–dielectric hyperbolic metamaterials *Photonics Res.* **7** 318–24
[7] Hou T *et al* 2019 Deep-learning-based phase control method for tiled aperture coherent beam combining systems *High Power Laser Sci. Eng.* **7** e59
[8] Teng S, Zhang Q, Wang H, Liu L and Lv H 2019 Conversion between polarization states based on metasurface *Photonics Res.* **7** 246–50
[9] Akram M, Ding G, Chen K, Feng Y and Zhu W 2020 Ultrathin single layer metasurfaces with ultra-wideband operation for both transmission and reflection *Adv. Mater.* **32** 1907308
[10] Akram M, Mehmood M, Bai X, Jin R, Premaratne M and Zhu W 2019 High efficiency ultrathin transmissive metasurfaces *Adv. Opt. Mater.* **7** 1801628
[11] Jing X, Chu C, Li C, Gan H, He Y, Gui X and Hong Z 2019 Enhancement of bandwidth and angle response of metasurface cloaking through adding antireflective moth-eye-like microstructure *Opt. Express* **27** 21766–77
[12] Wang H, Zheng J, Fu Y, Wang C, Huang X, Ye Z and Qian L 2019 Multichannel high extinction ratio polarized beam splitters based on metasurfaces *Chin. Opt. Lett.* **17** 052303
[13] Huault M *et al* 2019 A 2D scintillator-based proton detector for high repetition rate experiments *High Power Laser Sci. Eng.* **7** e60
[14] Koirala L, Park C, Lee S and Choi D 2019 Angle tolerant transmissive color filters exploiting metasurface incorporating hydrogenated amorphous silicon nanopillars *Chin. Opt. Lett.* **17** 082301
[15] Fu Y, Fei Y, Dong D and Liu Y 2019 Photonic spin Hall effect in PT symmetric metamaterials *Front. Phys.* **14** 62601
[16] Hanuka A, Wootton K, Wu Z, Soong K, Makasyuk I, England R and Schchter L 2019 Cumulative material damage from train of ultrafast infrared laser pulses *High Power Laser Sci. Eng.* **7** e7
[17] Fu Y, Xu Y and Chen H 2018 Negative refraction based on purely imaginary metamaterials *Front. Phys.* **13** 134206
[18] He Z, Zhu Y and Wu H 2018 Self-folding mechanics of graphene tearing and peeling from a substrate *Front. Phys.* **13** 138111
[19] Song Z, Chu Q, Shen X and Liu Q 2018 Wideband high-efficient linear polarization rotators *Front. Phys.* **13** 137803
[20] Shin D, Urzhumov Y, Jung Y, Kang G, Baek S, Choi M, Park H, Kim K and Smith D 2012 Broadband electromagnetic cloaking with smart metamaterials *Nat. Commun.* **3** 1213
[21] Ma H and Cui T 2010 Three-dimensional broadband ground-plane cloak made of metamaterials *Nat. Commun.* **1** 21

[22] Chen H, Zheng B, Shen L, Wang H, Zhang X, Zheludev N and Zhang B 2013 Ray-optics cloaking devices for large objects in incoherent natural light *Nat. Commun.* **4** 2652
[23] Alù A 2009 Mantle cloak: invisibility induced by a surface *Phys. Rev.* B **80** 245115
[24] Silveirinha M and Engheta N 2007 Theory of supercoupling, squeezing wave energy, and field confinement in narrow channels and tight bends using ε near-zero metamaterials *Phys. Rev.* B **76** 245109
[25] Wang J, Qu S, Xu Z, Ma H, Zhang J, Li Y and Wang X 2013 Super-thin cloaks based on microwave networks *IEEE Trans. Antennas Propag.* **61** 748–54
[26] Orazbayev B, Mohammadi Estakhri N, Beruete M and Alù A 2015 *Phys. Rev.* B **91** 195444
[27] Gharghi M, Gladden C, Zentgraf T, Liu Y, Yin X, Valentine J and Zhang X 2011 *Nano Lett.* **11** 2825
[28] Xu S, Xu H, Gao H, Jiang Y, Yu F, Joannopoulos J D, Soljačić M, Chen H, Sun H and Zhang B 2015 *Proc. Natl Acad. Sci. USA* **112** 7635
[29] Yang J, Huang C, Wu X, Sun B and Luo X 2018 *Adv. Opt. Mater.* **6** 1800073
[30] Wang C, Yang Y, Liu Q, Liang D, Zheng B, Chen H, Xu Z and Wang H 2018 *Opt. Express* **26** 14123